



MICROSTRUCTURAL EVOLUTION OF HIGH DENSITY W-CERMETS EXPOSED TO FLOWING HYDROGEN AT TEMPERATURES EXCEEDING 2000 K

William J. Carpenter^{1,2}, Kelsa M. Benensky^{1,3}, Marvin W. Barnes¹, and Dennis S. Tucker¹

¹Materials and Processes Laboratory, NASA Marshall Spaceflight Center, Huntsville, AL 35811

²Department of Metallurgical Engineering, South Dakota School of Mines and Technology, Rapid City, 57701

³Department of Nuclear Engineering, University of Tennessee, Knoxville, TN 37996

Nuclear thermal propulsion (NTP) shows promising potential for crewed space exploration by enabling high specific impulse and thrust. The development of NTP systems presents unique fuel material challenges due to requirements for high operating temperatures, exceeding 2500 K, and chemical compatibility with a hydrogen (H₂) propellant (coolant) during operation. NASA has been investigating ceramic-metal (cermet) fuels due to their high temperature capability and H₂ compatibility of the refractory metal matrix. For this study, subscale tungsten (W) cermet specimens, with 60 vol% zirconia surrogate (ZrO₂), were consolidated via spark plasma sintering (SPS). Sintered samples were tested at 2000°C for 60 minutes and 2500°C for 5 minutes in flowing H₂. After testing, as produced and tested specimens were cross sectioned for microstructural examination using optical microscopy, scanning electron microscopy, and microhardness in order to understand the stability of the bulk cermet microstructure under the different conditions. While the specimens retained structural integrity throughout testing with minimal mass loss, the microstructural investigation revealed H₂ attack and migration of ZrO₂ particles. Overall, the W matrix showed minimal grain growth and embrittlement as a result of testing.

I. INTRODUCTION

Nuclear thermal propulsion (NTP) is a promising technology for manned missions to Mars due to the capability for high specific impulse and reasonable thrust^{1,2}. In NTP systems, a nuclear reactor is used as a heat exchanger to transfer the energy generated from nuclear fission to directly heat a light weight propellant, typically H₂. One of the main challenges for the successful development of NTP systems is the fabrication of a viable fuel material which is capable of operation in a highly reducing environment (H₂) and temperatures exceeding 2230 °C (2500 K)^{3,4}. Composed of a refractory metal matrix and dispersed ceramic fuel particles (UO₂, UN, etc.), ceramic-metallic (cermet) fuels are under investigation by NASA for use in NTP environments. Tungsten (W) cermet fuels have shown capability for NTP applications, with the potential for high specific impulse, due to the high melting point (~3700 K), low vapor pressure, and H₂ capability of the W-matrix^{3,5,6}.

W-cermets were originally developed for NTP (and nuclear space power) applications as an alternative to the graphite-matrix fuel elements explored during the NERVA/Rover Program. Cermet fuel development was primarily undertaken by General Electric under the GE710 program⁷. However initial scoping studies and significant supporting development was also pursued under programs at Los Alamos National Laboratory⁸ Argonne National Laboratory⁹ and NASA Lewis Research Laboratory¹⁰. Throughout historic cermet development programs, cermet fabrication evolved from hot rolling of Mo-UO₂ plates to culminate in fabrication of net shape W-UO₂ hexagonal rod fuel elements via a multi-step sintering, diffusion bonding process. This multi-step net shape fabrication process consisted of: 1) sintering of near net-shape W alloy-UO₂ wafers via hot isostatic pressing (HIP), 2) element assembly via stacking wafers within a wrought cladding assembly composed of a structural W-housing and W-coolant channels, and 3) diffusion bonding to form a net shape fuel element (cladded, hexagonal rod elements with cooling channels) via HIP. While this process is energy intensive and complex, fabrication of elements via this method allowed for incorporation of the design features associated with highest fuel performance and stability.

Recent studies have shown that near theoretical density cermet wafers with high ceramic volume loadings may be produced using spark plasma sintering (SPS) at much lower process temperatures^{3,5,11,12} than previously achievable through conventional HIP processes^{13,14}. This is desirable for both more affordable fuel manufacture, as well as to limit pre-mature degradation of the UO₂ feedstock particles, which are susceptible to reduction when exposed to high temperatures for long durations such as during conventional sintering processes. NASA has been investigating SPS as an alternate fabrication route to produce cermet wafers to be utilized in the net shape manufacture of fuel elements¹⁵. This has included fabrication of W-ZrO₂ (surrogate) and W-UO₂ fuel wafers with large spherical ceramic fuel particles (~100 - 250 μm diameter) in an attempt to improve the material's robustness when exposed to intense thermal stresses during high temperature exposure and thermal cycling¹⁶. However, performance of SPS-fabricated W-cermet

wafers with desirable microstructures in a hot H₂ environment has not been fully assessed or reported.

In this study, results from recent testing of SPS-fabricated, W-matrix, 60-vol% spherical ZrO₂ particle loaded cermet in a hot H₂ environment is presented. Separate samples were tested under two test conditions, with one at 2000 °C for 60 minutes and one at 2500 °C for 5 minutes. These temperatures were chosen to investigate bulk material stability under the minimum operating requirements for the hot end of the fuel (2000 °C, 60 minutes) and its potential for ultra-high temperature operation (2500 °C, 5 minutes). In the later case, it was of particular interest to understand bulk material stability when incorporating a spherical ceramic particle rather than angular powders. Previous attempts to test cermets sintered with angular ceramic particle feedstock have resulted in catastrophic material failure and loss of structural stability, which was attributed to intense stresses caused by difference in coefficient of thermal expansion (CTE) mismatch and high angle grain boundary interfaces of the ceramic and metal phases¹⁷. Therefore, material survivability was assessed as preservation of structural integrity of tested wafers and retention of the ceramic phase within the bulk microstructure. In addition, hot H₂ tests performed in this study allowed for an initial insight into anticipated degradation mechanisms, changes in mechanical properties of the fuel as a result of hot H₂ exposure. Lessons learned from these studies can be utilized to optimize future SPS-manufacture parameters of fuel wafers, as well as guide more detailed studies which probe lifetime limiting degradation phenomena.

II. EXPERIMENTAL

W-matrix cermets were fabricated using a two-step powder blending, spark plasma sintering (SPS) process previously described by Tucker *et al.*³ This process is utilized to increase the uniformity of dispersion of ceramic within the metal matrix and minimize possibility of ceramic particle agglomeration. ZrO₂ was selected as a surrogate for UO₂. Blended powders were sintered into 20 mm diameter, 25 g pellets using SPS parameters of 1700 °C, 50 MPa, 10 minute dwell time to ensure a near theoretical density pellet with a low porosity metal matrix and a diffusion bonded matrix-particle interface.

After sintering, samples were prepped for testing by grinding flat with silicon carbide paper until the carbide reaction layer on the top and bottom faces was removed (~ 150 μm thickness). Samples were cleaned with deionized water, degassed in ethanol, dried, measured, and weighed using a precision balance. Prepared samples were transferred and loaded into the compact fuel element environmental test¹⁸ (CFEET), a custom H₂ induction furnace, for high temperature, flowing H₂ exposure. The furnace design allows for the passage of H₂ flow through

a heating assembly in which samples are radiatively heated to temperature by a W susceptor. Samples are centered within the susceptor on an inert ZrO₂ crucible plate, schematic drawing shown in figure 1. In the furnace design, H₂ enters the furnace at a rate of 0.500 standard liters per minute (SLPM) throughout the duration of testing, including heating and cooling. Samples are ramped to temperature at a rate of ~400 °C/minute, held at temperature for the desired duration, and subsequently ramped down to room temperature at a rate of ~400 °C/minute using manual control of the power supplied to the induction furnace. During testing, sample temperature is measured using a non-contact 2-color optical pyrometer (Ircan Modline 5R). Cool down rate is limited by convection once zero power is achieved and an argon purge is utilized to cool the sample to room temperature for removal and inspection.

Tested samples were compared to a reference as fabricated cermet during microstructural analysis. After hot H₂ testing, all samples were cross sectioned in half and the exposed surface ground flat to 4000 grit silicon carbide paper. The samples were mechanically polished to 1 μm using diamond suspension. The samples were cleaned after each grit with water and soap, and cleaned after each polishing step with water, soap, and ethanol. After the initial investigation into the microstructure, the samples were etched according to ASM Volume 9 (reference¹⁹) with Murakami's Reagent to analyze the grain size within the W matrix using the line intercept method²⁰⁻²².

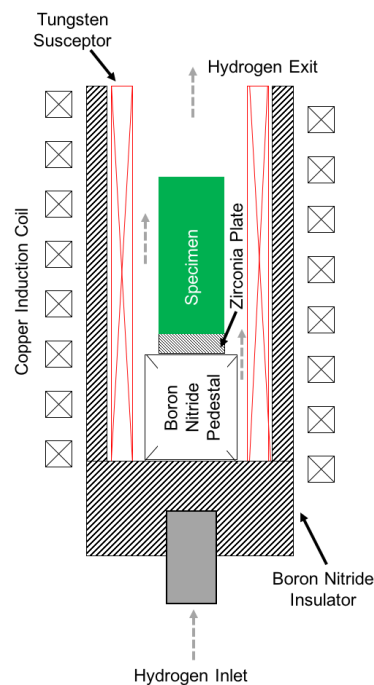


Fig. 1. Schematic drawing of CFEET heating assembly and flow path.

Optical microscopy (OM) was performed before and after etching to investigate the microstructure, with efforts placed on: the W matrix, the W- ZrO₂ interface, and the ZrO₂ particles. Scanning electron microscopy (SEM) was used in backscattered mode to analyze the compositional stability of the tested samples. Energy Dispersion Spectroscopy (EDS) was used to determine chemical composition distribution throughout the cermet.

Vickers microhardness tests were performed on the samples after polishing to 1 μm. The load was set at 0.3kg and 10 second dwell time. All tests were performed within the metal matrix to understand the mechanical behavior of the W matrix after hot H₂ testing.

III. RESULTS AND DISCUSSION

I.A. Optical Microscopy Results

I.A.1. Bulk Microstructural Investigation

The typical as-fabricated microstructure (fig. 2) exhibits diffusion bonding of the ceramic particles with the metal matrix, good uniformity of dispersion of the ceramic particles within the matrix with minimal particle interconnectivity, and high matrix density. The ceramic ZrO₂ particles exhibit cracking near ZrO₂-ZrO₂ interfaces, however most particles are intact with no noticeable cracking or porosity.

Figures 3 and 4 show the cermet microstructure after hot H₂ exposure at 2000° C and 2500° C respectively. Both samples survived the hot H₂ testing with maintained structural integrity and retention of dispersed ceramic particles. Compared to the as-fabricated microstructure, the ZrO₂ particles within the tested samples contained cracking, but all cracking is arrested by the W matrix and samples retain the ZrO₂ at full density. Within both samples, exposure to the hot H₂ environment degraded the ZrO₂ particles along the grain boundaries, leading to grain pullout of the ZrO₂ during polishing. The matrix exhibits signs of porosity in both tested samples. Most notable in Figure 5, pores appear along the grain boundaries within the particles, indicative of either micropore accumulation or gas bubble formation. Similar microstructural features are observed in high burnup UO₂, which has been attributed to the buildup of gaseous fission products which nucleate gas bubbles which evolve to form a porous, high burn-up microstructure at the grain boundaries^{23,24}.

Since as-received ceramic particles are near theoretical density, it is thought that the reduction reaction of $ZrO_2 \rightarrow ZrO_{2-x} + \frac{1}{2}x O_2$, may attribute to the formation of free oxygen gas (O₂) within the ceramic microstructure. At high temperatures, free O₂ may have enough diffusivity to migrate quickly to the grain boundaries and accumulate within gas bubbles once a critical

concentration is achieved. However, visible formation of intragranular pores are also present throughout the ceramic microstructure, which may be indicative that free O₂ is also present in high enough concentrations to form stable in bubbles within the grains. ZrO₂ degradation could be further exacerbated by its low thermal conductivity creating a thermal gradient throughout the large ceramic particles, as well as a CTE mismatch between the W and ZrO₂ interface^{25,26}.

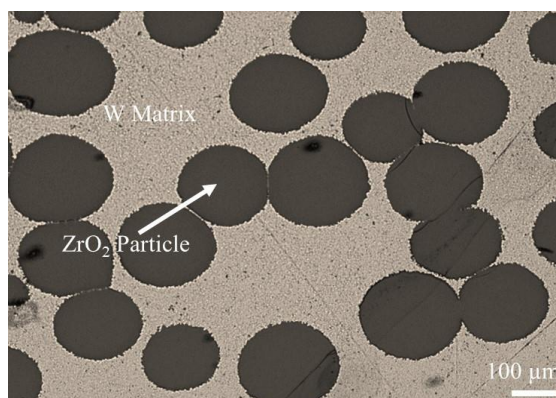


Fig. 2. The as-fabricated microstructure of a representative W-60 vol% ZrO₂ cermet using optical microscopy. The tungsten matrix exhibits a favorable microstructure with minimal closed porosity, indicating a near theoretical density matrix. ZrO₂ particles are retained within the W matrix with limited apparent cracking and no matrix cracking. The particles exhibit a diffusion bonded interface with the W matrix and good dispersion throughout the matrix.

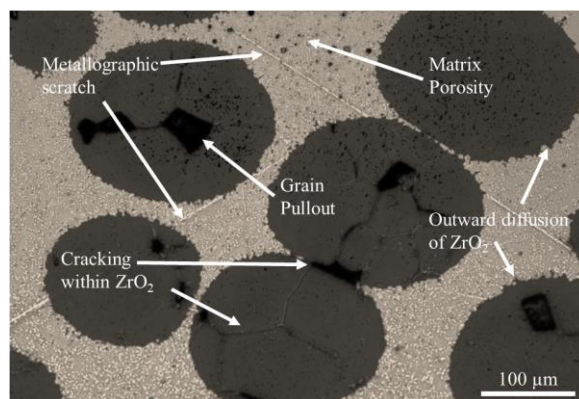


Fig. 3. Optical micrograph of W-ZrO₂ cermet microstructure after exposure to flowing H₂ at 2000° C for 60 minutes. ZrO₂ particles are completely retained within the W matrix without any matrix cracking (loss of structural integrity) but with porosity in the matrix. Ceramic degradation is observed with cracking within the ZrO₂ along the grain boundaries. This resulted in grain pullout within the ZrO₂ during polishing. Continued diffusion of ZrO₂ outward from the particles into the matrix is observed at the interfaces.

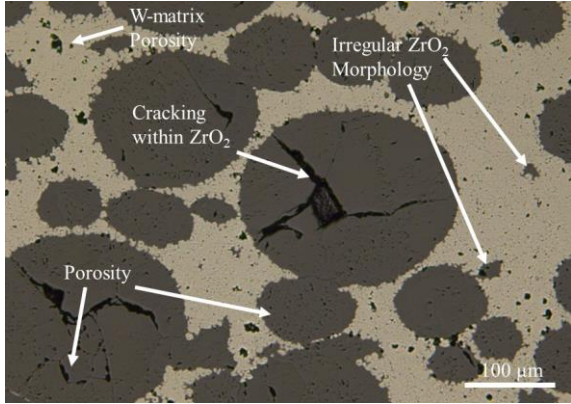


Fig. 4. Optical micrograph of W-ZrO₂ cermet microstructure after exposure to flowing H₂ at 2500° C for 5 minutes. Cracking and porosity are present within the ZrO₂ particles. The porosity is present at grain boundaries and throughout the grains. New irregular ZrO₂ morphologies and porosity are present within the W matrix.

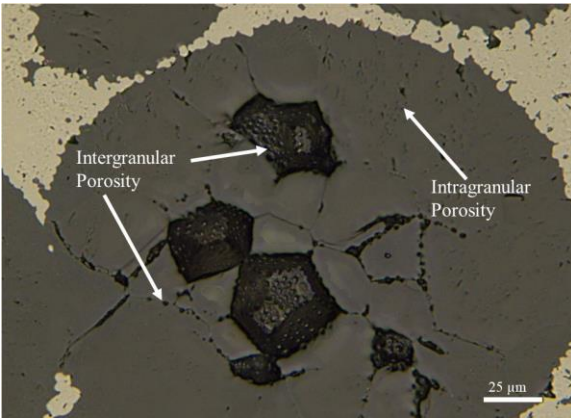


Fig. 5. Optical micrograph of ZrO₂ degradation within the 2500° C sample. Image obtained by z-stacking images to obtain full depth of view. Porosity concentrated at grain boundaries may be indicative of free gas formation and nucleation within the particle.

I.A.2. Grain Size and Microhardness Analysis

Tested samples maintained a similar grain size in comparison to the as-fabricated samples (Table I). Indication of recrystallization appeared in the 2000° C sample with large grains throughout the sample, shown in Figure 6. The recrystallization combines grains leading to the embrittlement of the W-matrix. The test temperatures exceeded recrystallization temperature of W (1200 - 1400 °C)²⁷, however the sample exposed to 2500 °C did not exhibit evidence of recrystallization. This could be the result of the sample not being exposed to the testing temperature (5 minutes) for as long duration as the 2000 °C sample (60 minutes). Previous work on the sintering of W has used a nano-dispersion of rare earth to maintain a finer microstructure via the grain pinning mechanism to

limit grain growth²⁸⁻³⁰. However, it is unclear if these additions will be stable when exposed to a high temperature H₂ environment.

Table I. Average grain size measurements using Line Intercept Method.

Sample	Grain Size (μm)
As Fabricated	4.44 ± 0.26
2000° C, 60 min.	7.77 ± 0.57
2500° C, 5 min.	5.58 ± 0.47

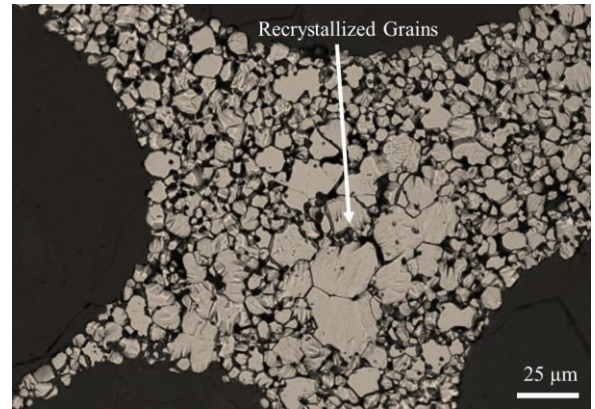


Fig. 6. Large grains resulting from W-matrix recrystallization after exposure to 2000 °C for 60 minutes. Uniform recrystallization did not occur, but rather only for discrete locations within the cermet.

The microhardness indicates that the W matrix goes through a change of mechanical properties as a result of the hot H₂ testing. In Table II, the tested samples significantly increase in hardness compared to the as fabricated sample. The hardening within the matrix could be attributed to H₂ embrittlement²⁷. However, change in mechanical properties of the ZrO₂ particles was not assessed, it is unclear if ZrO₂ degradation is predicted to play any role in apparent matrix hardening. Previous studies have shown UO₂ exhibits a decrease in hardness and Young's modulus as a result of increased porosity³¹. With increased degradation of the ZrO₂, the fuel element could lose significant strength and may lead to unique modes of failure.

Table II. Microhardness of W matrix for tested and as fabricated samples. The samples show an increase in hardness as a result of thermal cycling.

Sample	Microhardness (0.3HV)
As Fabricated	184 ± 34.7
2000° C, 60 min.	229 ± 35.7
2500° C, 5 min.	271 ± 26.2

I.B. Scanning Electron Microscopy and Energy Dispersive Spectroscopy

Scanning electron microscopy and energy dispersive x-ray spectroscopy was utilized to assess if any compositional evolution of the cermet was incurred

during operation. Through historic cermet development programs, known degradation mechanisms of UO_2 containing cermets for NTP applications are well characterized and reviewed in detail elsewhere³². For brevity, they are summarized as the following:

- 1) High temperature reduction of UO_2 to form free metal (U), which attacks (weakens) cermet grain boundaries and interacts with propellant to form high volume expansion hydrides.
- 2) Ratcheting and loss of structural integrity of cermet due to difference in thermal expansion of metal matrix and ceramic particle and incurred thermal stresses during one or more thermal cycles.
- 3) Removal of interconnected ceramic particles due to high diffusivity at temperature and incompatibility with the H_2 propellant.

Figure 7 shows back scattered electron (BSE) image of a representative W-ZrO₂ microstructures after exposure. The BSE imaging shows that the morphology of the W-ZrO₂ interface becomes highly irregular as a result of 2500 °C exposure due to diffusion of ZrO₂ into the matrix. Despite the irregular interface no secondary phases could be identified upon initial inspection, which is desirable to ensure long lifetime at operating temperature. Isolated regions of irregular ZrO₂ morphology are most likely due to outward diffusion of embedded particles below the sample surface. Previous studies on the characterization of W-cermet microstructures fabricated using SPS have shown that at sintering temperatures exceeding 1700 °C, free U migration was evident at the W-UO₂ interface. Future work should aim to characterize tested cermets using higher resolution techniques, such as atom probe tomography to identify the compositional stability and evolution at the interface.

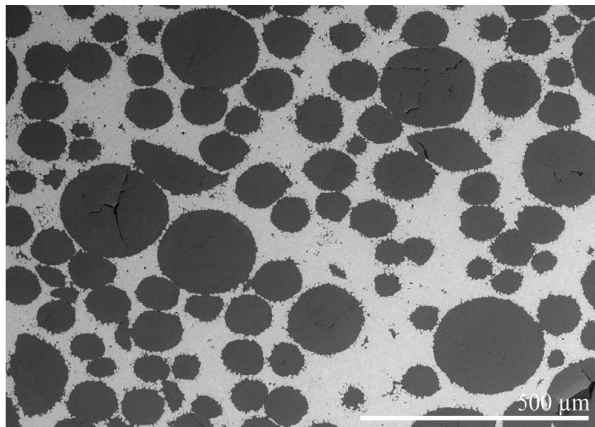


Fig. 7. Representative BSE image of cermet microstructure tested at 2500 °C for 5 minutes. No secondary phases are evident and intergranular porosity is confined to ZrO₂ particles.

IV. CONCLUSIONS

While previous W-cermets sintering using angular powder feedstocks performed poorly when exposed to 2500 °C H_2 conditions¹⁷, W-60 vol% ZrO₂ cermet samples with desirable microstructures maintained structural integrity and retained ceramic particles for hot H_2 exposure conditions of 2000 °C, 60 minutes and 2500 °C, 5 minutes. For both samples tested, cermets were able to retain bulk structural integrity and no cracking was exhibited by the W matrix. However, the ceramic ZrO₂ particles exhibited significant cracking after thermal cycling, localized degradation along the grain boundaries, and formation of intergranular pores.

Preliminary scoping studies using SEM imaging and EDS spectra analysis show evolution in ZrO₂ morphology and particle migration. However, initial inspection did not show conclusive evidence of secondary phase formation. The microhardness data shows that in all test cases the W matrix increases in hardness, despite minor grain growth. This is attributed to matrix embrittlement as a result of H_2 exposure. Further efforts should be aim to confirm, understand the oxygen transportation degradation mechanism of the ceramic fuel particles, as well as anticipated mechanical evolution of the W matrix. Special emphasis should be placed on understand the impact of microstructural, property evolution on expected fuel thermal mechanical performance and lifetime. To assist in this effort, detailed studies should be undertaken to provide a quantitative analysis of the oxygen to metal ratios within the ceramic as a function of exposure temperature and duration, as well as to investigate the formation of pores within the ceramic and determine if their formation is due to void or gas bubble nucleation. Future work is also needed to test cermets to failure in order to understand expected lifetime under various thermal cycling conditions and exposure temperatures. In addition to detailed analysis of intergranular porosity observed in ZrO₂ particles, characterization of free metal migration and onset of secondary phase formation within the ceramic will be necessary upon exposure to more intense operating conditions and leading up to cermet failure.

ACKNOWLEDGMENTS

I would like to express my gratitude to my fellow co-workers, specifically to Marvin Barnes, Omar Rodriguez, and Tafton Hastings. This work was performed in part under NASA Grant #NNX15AQ35H (KMB) and the NASA Pathways Program (WJC). This work was funded through the NTP project at NASA Marshall Spaceflight Center.

REFERENCES

1. Borowski, S., Corban, R., McGuire, M. & Beke, E. Nuclear thermal rocket/vehicle design options for

- future NASA missions to the moon and Mars. *Sp. Programs Technol. Conf. Exhib.* (1993). doi:10.2514/6.1993-4170
2. Lawrence, T. J. Nuclear Thermal Rocket Propulsion Systems, Iaa White Paper. *Organization* 18 (2005).
 3. Tucker, D. S., Barnes, M. W., Hone, L. & Cook, S. High density, uniformly distributed W/UO₂ for use in Nuclear Thermal Propulsion. *J. Nucl. Mater.* **486**, 246–249 (2017).
 4. Borowski, S. K., Mccurdy, D. R. & Packard, T. W. Nuclear Thermal Propulsion (NTP): A Proven Growth Technology for Human NEO/Mars Exploration Missions. *Glob. Sp. Explor. Conf.* 1–15 (2012). doi:10.1109/AERO.2012.6187301
 5. Webb, J. A. & Charit, I. Fabrication of cermetts via spark-plasma sintering for nuclear applications. *Jom* **66**, 943–952 (2014).
 6. Broadway, J., Hickman, R. & Mireles, O. The Manufacture of W UO₂ Fuel Elements for NTP Using the Hot Isostatic Pressing Consolidation Process NASA Advanced Exploration Systems (AES) Program. (2012).
 7. *710 High-Temperature Gas Reactor Program Summary Report.* (1968).
 8. Lenz, W. H., Peterson, C. E. & Taub, J. M. *The Processing and Testing of Mo-UO₂ Cermet Fuel Elements.* (1960).
 9. *Nuclear Rocket Program: Terminal Report, ANL-7236.* (1968).
 10. Sikora, P. F. & Blankenship, C. P. *Evaluation of Processes for Fabricating Tungsten-Uranium Dioxide Honeycomb Configurations, NASA TM X-1445.* (1967).
 11. Zhong, Y. *et al.* Spark Plasma Sintering of Fuel Cermetts for Nuclear Reactor Applications. *MRS Proc.* **1383**, mrsf11-1383-a01-08 (2012).
 12. O'Brien, R. C. & Jerred, N. D. Spark Plasma Sintering of W-UO₂ cermetts. *J. Nucl. Mater.* **433**, 50–54 (2013).
 13. Hickman, R., Panda, B. & Shah, S. Fabrication of High Temperature Cermet Materials for Nuclear Thermal Propulsion. (2005).
 14. Hickman, R., Broadway, J. & Mireles, O. Fabrication and Testing of CERMET Fuel Materials for Nuclear Thermal Propulsion. 37 (2006).
 15. Barnes, M. W., Tucker, D. S. & Benensky, K. Demonstration of Subscale Cermet Fuel Specimen Fabrication Approach Using Spark Plasma Sintering and Diffusion Bonding. 5–8 (2018).
 16. Baker, R., Daniel, J. & Lackey, W. Basic Behavior and Properties of W-UO₂ CERMETS Final Report. (1965).
 17. Hickman, R., Broadway, J., Trent, D. & Dziubanek, A. Hot Hydrogen Testing of Tungsten-Uranium Dioxide(W-UO₂) CERMET Fuel Materials for Nuclear Thermal Propulsion. in *AIAA Joint Propulsion Conference* (2014).
 18. Benensky, K., Barnes, M. W., Romnes, C. & Hickman, R. Operational Characterization and Testing of NASA MSFC's Compact Fuel Element Environmental Test (CFEET). in *2018 Nuclear and Emerging Technologies for Space*
 19. Vander Voort, G. F. *ASM Handbook, Volume 09 - Metallography and Microstructures.* (2004).
 20. ASTM E112-13, Standard Test Methods for Determining Average Grain Size. (2013).
 21. Vashi, U. K., Armstrong, R. W. & Zima, G. E. The Hardness and Grain size of consolidated fine tungsten powder. *Metall. Trans.* **1**, 1769–1771 (1970).
 22. El-Atwani, O. *et al.* Multimodal grain size distribution and high hardness in fine grained tungsten fabrication by spark plasma sintering. *Mater. Sci. Eng. A* **528**, 5670–5677 (2011).
 23. Rondinella, V. V. & Wiss, T. The high burn-up structure in nuclear fuel. *Mater. Today* **13**, 24–32 (2010).
 24. Noirot, J., Pontillon, Y., Yagnik, S. & Turnbull, J. A. Post-irradiation examinations and high-temperature tests on undoped large-grain UO₂ discs. *J. Nucl. Mater.* **462**, 77–84 (2015).
 25. Mistarihi, Q., Umer, M. A., Kim, J. H., Hong, S. H. & Ryu, H. J. Fabrication of ZrO₂-based nanocomposites for transuranic element-burning inert matrix fuel. *Nucl. Eng. Technol.* **47**, 617–623 (2015).
 26. Stewart, M. E. M. & Schnitzler, B. G. A Comparison of Materials Issues for Cermet and Graphite- Based NTP Fuels. in 1–13 (2013).
 27. Samal, P. K. & Newkirk, J. W. *ASM Handbook, Volume 7 - Powder Metallurgy* (2015). (2015).
 28. Luo, L. *et al.* Microstructure and performance of rare earth element-strengthened plasma-facing tungsten material. *Sci. Rep.* **6**, 1–10 (2016).
 29. Ding, X.-Y. *et al.* Chemical Synthesis and Oxide Dispersion Properties of Strengthened Tungsten via Spark Plasma Sintering. *Materials (Basel)*. **9**, 879 (2016).
 30. Vilémová, M. *et al.* Properties of Ultrafine-Grained Tungsten Prepared by Ball Milling and Spark Plasma Sintering. *Appl. Mech. Mater.* **821**, 399–404 (2016).
 31. Cappia, F. *et al.* Microhardness and Young's modulus of high burn-up UO₂fuel. *J. Nucl. Mater.* **479**, 447–454 (2016).
 32. Haertling, C. & Hanrahan, R. J. Literature review of thermal and radiation performance parameters for high-temperature, uranium dioxide fueled cermet materials. *J. Nucl. Mater.* **366**, 317–335 (2007).